View metadata, citation and similar papers at core.ac.uk
brought to you by CORE
provided by Elsevier - Publisher Connector

Biochimica et Biophysica Acta 1808 (2011) 2665–2673

Contents lists available at ScienceDirect

Biochimica et Biophysica Acta

journal homepage: www.elsevier.com/locate/bbamem

Cyclotide–membrane interactions: Defining factors of membrane binding, depletion and disruption

Robert Burman [a,1], Adam A. Strömstedt [a,1], Martin Malmsten [b], Ulf Göransson [a,*]

[a] Division of Pharmacognosy, Department of Medicinal Chemistry, Uppsala University, Box 574, BMC, SE-751 23 Uppsala, Sweden
[b] Department of Pharmacy, Uppsala University, Box 580, BMC, SE-751 23 Uppsala, Sweden

ARTICLE INFO

Article history:
Received 13 April 2011
Received in revised form 23 June 2011
Accepted 1 July 2011
Available online 20 July 2011

Keywords:
Cyclotide
Cycloviolacin O2
Kalata
Membrane
Phosphatidylethanolamine
Lipid extraction

ABSTRACT

The cyclotide family of plant-derived peptides is defined by a cyclic backbone and three disulfide bonds locked into a cyclic cystine knot. They display a diverse range of biological activities, many of which have been linked to an ability to target biological membranes. In the current work, we show that membrane binding and disrupting properties of prototypic cyclotides are dependent on lipid composition, using neutral (zwitterionic) membranes with or without cholesterol and/or anionic lipids. Cycloviolacin O2 (cyO2) caused potent membrane disruption, and showed selectivity towards anionic membranes, whereas kalata B1 and kalata B2 cyclotides were significantly less lytic towards all tested model membranes. To investigate the role of the charged amino acids of cyO2 in the membrane selectivity, these were neutralized using chemical modifications. In contrast to previous studies on the cytotoxic and antimicrobial effects of these derivatives, the Glu6 methyl ester of cyO2 was more potent than the native peptide. However, using membranes of *Escherichia coli* lipids gave the opposite result: the activity of the native peptide increased 50-fold. By using a combination of ellipsometry and LC-MS, we demonstrated that this unusual membrane specificity is due to native cyO2 extracting preferentially phosphatidylethanolamine-lipids from the membrane, i.e., PE-C16:0/cyC17:0 and PE-C16:0/C18:1.

© 2011 Elsevier B.V. All rights reserved.

1. Introduction

Cyclotides constitute a family of plant-derived peptides with an exceptionally stable structure [1,2]. They consist of approximately 30 amino acids with their N- and C-termini connected via an ordinary peptide bond, resulting in a circular backbone. The structure is reinforced by three disulfide bonds arranged in a cystine knot at its core. This structural motif, the so-called cyclic cystine knot (CCK), forces the relatively large number of hydrophobic residues of the cyclotide sequence to be exposed at the surface of the molecule, resulting in pronounced amphiphilic properties. A structural twist of the cyclic backbone, i.e., the presence or absence of a *cis*-Pro residue, divides the growing family of cyclotides into two subfamilies, the Möbius and the bracelet cyclotides, respectively (Fig. 1).

The unique structure of the cyclotides has been associated with a number of reported biological activities, including cytotoxic [3], hemolytic [4,5], anti-HIV [6], anthelmintic [7], anti-fouling [8], antimicrobial [9,10] and insecticidal activity [11]. These effects – at least the latter ones – indicate that the biological role of cyclotides within the expressing plants is that of host defense. As outlined below, recent studies demonstrate that there is a strong connection between structure and activity of cyclotides, and that the interaction between the cyclotide and the lipid membrane of the target cell is the major cause for activity.

The bracelet cyclotide cycloviolacin O2 (cyO2) is the most potent cyclotide that have been tested for cytotoxic and antimicrobial effects [3,9,12]. In light of the division into subfamilies based on the structural twist, it is noteworthy that cyO2 is characterized by two cationic Lys residues in loop 5, and a short hydrophobic alpha helix in loop 3, whereas prototypic Möbius cyclotides such as kalata B1 and kalata B2 (kB1/kB2) lack these features (Fig. 1). Triggered by these results, cyO2 has been subjected to chemical modifications to investigate the impact of the charged residues. Up to a 7-fold decrease in cytotoxic activity was seen after masking the cationic side chains of the single Arg and the two Lys residues (by reaction with 1,2-cyclohexanedione or by acetylation, respectively). Surprisingly however, masking of the single negatively charged residue, a conserved Glu, resulted in a 48-fold decrease [12].

In analogy to the cytotoxic structure-activity relationship, cyO2 was recently shown to be the most potent bactericidal cyclotide when screening a smaller set of cyclotides (including kB1 and kB2) [9]. In that assay, the Glu modification caused a loss of activity against the main target *Salmonella enterica* serovar Typhimurium LT2, as did

Abbreviations: cyO2, cycloviolacin O2; DOPA, Sodium 1,2-dioleoyl-*sn*-glycero-3-phosphate; DOPC, 1,2-dioleoyl-*sn*-glycero-3-phosphocholine; kB1, kalata B1; kB2, kalata B2; PE, Phosphatidylethanolamine

* Corresponding author. Tel.: +46 18 4715031; fax: +46 18 509101.
E-mail addresses: Robert.Burman@fkog.uu.se (R. Burman), Adam.Stromstedt@fkog.uu.se (A.A. Strömstedt), Marin.Malmsten@farmaci.uu.se (M. Malmsten), Ulf.Goransson@fkog.uu.se (U. Göransson).

[1] These authors contributed equally to this work and should be considered as joint first authors.

0005-2736/$ – see front matter © 2011 Elsevier B.V. All rights reserved.
doi:10.1016/j.bbamem.2011.07.004

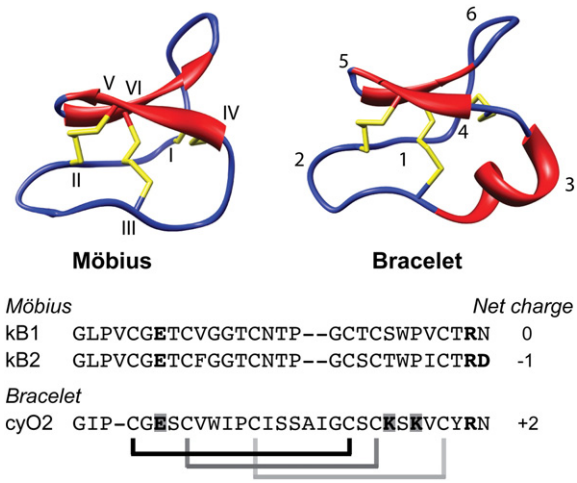

Fig. 1. Ribbon structures of the Möbius kalata B1 and the bracelet cycloviolacin O2 and cyclotide sequences. Note the unique features of the cyclic cystine knot (CCK) motif: a cyclic backbone and three stabilizing disulfide bonds arranged in a cystine knot, i.e., two disulfide bonds (I–IV, II-V) form a ring together with their interconnecting backbones, and the third disulfide bond (III–VI) is threaded through that ring. The sequences between cysteines, the sequence loops (marked as 1–6 in the structure to the right), are more or less variable. The sequences of the cyclotides in focus in the current work are shown below: kalata B1 (kB1), kalata B2 (kB2), and cycloviolacin O2 (cyO2). The brackets highlight the CCK-motif; charged residues are in bold. (PDB ID: 1NB1 and 2KNM.)

the Lys modification, while some activity was retained for the Arg modified cyO2.

It is becoming increasingly evident that the interaction of prototypic cyclotides with the lipid membrane is crucial for activity [13]. But the biophysical aspects of that interaction are poorly understood. Binding studies using surface plasmon resonance have demonstrated that some cyclotides (including kB1) bind to lipid membranes [14], while liposome leakage studies have demonstrated the lytic effect of cyO2 [13]. It has also been shown that cyclotides bind to dodecylphosphocholine micelles through a combination of electrostatic and hydrophobic interactions [15,16]; and that prototypic cyclotides of the two Möbius and bracelet subfamilies (kB1 and cyO2, respectively) bind to the micelle surfaces with different orientation [17]. Moreover, recent studies postulate that the cyclotide kB1 disrupt membranes by the formation of multimeric pores [18,19].

The aim of the present study was to assess the interplay between cyclotide membrane binding and disruption. Prototypic cyclotides from the two subfamilies were used: the Möbius kB1 and kB2, and the bracelet cyO2. CyO2 was subjected to chemical modifications, targeting positively and negatively charged residues, to reveal additional mechanistic information. Membrane interactions of these cyclotides were studied by a combination of fluorescence spectroscopy, ellipsometry, and circular dichroism, in order to investigate the dependence of membrane affinity and lytic properties on membrane composition, electrostatics, and peptide structure.

2. Materials and methods

2.1. Chemicals

Phospholipids used were 1,2-dioleoyl-*sn*-glycero-3-phosphocholine (DOPC) and sodium 1,2-dioleoyl-*sn*-glycero-3-phosphate (DOPA) both of >99% purity, and a polar lipid extract from *Escherichia coli* (containing 67 mol% phosphatidylethanolamine, 23 mol% phosphatidylglycerol, and 10 mol% diphosphatidylglycerol) obtained from Avanti Polar Lipids (Alabaster, AL). Cholesterol (>99%) was obtained from Sigma-Aldrich (Steinheim, Germany), while poly-L-lysine (106–206 kDa) was from Sigma-Aldrich (St. Louis, MO). Water used was from a Millipore Milli-Q Plus 185 ultra-pure water system. Other chemicals were of analytical grade. If not stated otherwise, measurements were performed at 37 °C in 10 mM Tris buffer at pH 7.4, containing 5 mM glucose (ionic strength 0.006).

2.2. Plant material and extraction

Kalata B1 and B2 (kB1 and kB2) were isolated from *Oldenlandia affinis* D.C. (Rubiaceae), and cycloviolacin O2 (cyO2) was isolated from *Viola odorata* L. (Violaceae), as previously described [20]. Briefly, the dried plant material was extracted using 60% methanol in water, followed by liquid–liquid extraction with dichloromethane. Polar substances in the extracts were removed by loading the aqueous phase onto C18 material, which was washed with 30% methanol (aq) followed by elution of the cyclotides with methanol. The cyclotide containing fraction was concentrated, diluted with water and subjected to preparative reverse phase (C18) HPLC for isolation of individual cyclotides, to a final purity of >95%.

2.3. HPLC

An ÄKTA basic HPLC system equipped with a UV-detector (Amersham Biosciences, Uppsala, Sweden) was used for all HPLC experiments. Cyclotides were detected at 215, 254, and 280 nm. A ReproSil-Pur C18-AQ column (250 × 20 mm i.d., 10 μm, 300 Å) was used for preparative HPLC of the plant extracts, using a linear gradient from 10% acetonitrile in 0.05% trifluoroacetic acid (buffer A) to 60% acetonitrile in 0.045% trifluoroacetic acid (buffer B) over 45 min at a flow rate of 5.0 mL/min. To further purify native and modified peptides, an ACE C18 column (250 × 10 mm i.d., 5 μm, 300 Å) or a Vydac Everest C18 column (250 × 4.6 mm i.d., 5 μm, 300 Å) was used with a linear gradient from 30% to 70% buffer B over 60 min at a flow rate of 4.0 or 1.0 mL/min, respectively.

2.4. Chemical modifications

The Glu residue of cyO2 was esterified by slowly adding 1.0 mL of acetyl chloride to 6.0 mL of dry methanol [21], stirring the mixture at room temperature for 5 min, then adding the mixture to 3.0 mg of dry peptide before incubation at room temperature for 1 h, and finally quenching the reaction by adding 13 mL of water. For acetylation of the two Lys residues, 1.8 mg of cyO2 was dissolved in 3 mL of 50 mM NH_4HCO_3, adding the mixture to 30 μL acetic acid anhydride in 450 μL dry methanol [22], and then incubating the mixture at room temperature for 2 min, before quenching the reaction by adding 6.0 mL of water. After quenching, the products of all the reactions were immediately purified by HPLC to avoid side reactions. The isolated peptide derivatives, cyO2-Glu and cyO2-Lys showed an increase in mass of 14 and 84 Da, respectively. The selectivity of the chemical modifications was confirmed by MS/MS (Q-Tof Micro™; Waters, Milford, MA). The purity of the native peptides was determined by analytical RP-HPLC (Phenomenex C18, 250 × 4.6 mm i.d., 5 mm, 300 Å) using a linear gradient from buffer A to B. All peptides were >95% pure.

2.5. Cytotoxicity assay

The cytotoxicity of kB1, kB2, and cyO2 was analyzed using the lymphoma U-937 GTB, colon adenocarcinoma, HT29, and colorectal cancer cell line Ht116 in the fluorometric microculture cytotoxicity assay (FMCA) [23,24]. The FMCA is a cell viability assay used for measurement of the cytotoxic and/or cytostatic effect *in vitro*, based on hydrolysis of fluorescein diacetate (FDA) by esterases in cells with intact plasma membranes.

Peptides were dissolved in 10% ethanol and dilution series were prepared in V-shaped, 96-well microtiter plates (Nunc, Roskilde, Denmark) using 20 μL of peptide test solution per well. Also, six blank wells (200 μL per well of cell-growth medium) and six solvent-control wells (20 μL per well of 10% ethanol) were prepared on each microtiter plate. Tumor cells suspended in cell-growth medium were dispensed on the microtiter plates (20,000 cells/180 μL per well) and incubated for 72 h at 37 °C and 5% CO_2.

The cells were washed with PBS, and fluorescein diacetate added to each well after 40 min. The generated fluorescence was measured using a scanning fluorometer (excitation/emission wavelengths, 485/538 nm) (Fluoroscan II, Labsystems OY, Helsinki, Finland). IC_{50} values were calculated by non-linear regression in GraphPad Prism 4 (GraphPad Software, Inc., San Diego, CA, USA).

2.6. Liposome preparation

Dry lipid films (DOPC, DOPC/cholesterol (60/40 mol/mol), DOPC/DOPA (50/50 mol/mol), or *E. coli* lipid extract) were formed on flask walls by dissolving dry phospholipids in chloroform, followed by evaporation under a nitrogen gas flow and subsequently placed in vacuum overnight at room temperature. The lipid films were then resuspended in 100 mM 5(6)-carboxyfluorescein (Acros Organics, Geel, Belgium)(CF) in 10 mM Tris, pH 7.4, and subjected to 10 cycles of freezing in liquid nitrogen and thawing at 60 °C while vortexing.

Polydispersity and lamellar structures were reduced by repeated extrusion through 100 nm polycarbonate membranes mounted in a LipoFast mini-extruder (Avestin, Ottawa, Canada), and separated from un-trapped CF by gel filtration on a Sephadex G-25 column (Amersham Biosciences, Uppsala, Sweden). Alternatively, for ellipsometry and *E. coli* liposome preparation, the dried phospholipid films were re-suspended in Tris buffer at 50–60 °C while stirring for 30 min, to a concentration of 10 mM. The suspension was then vortexed and repeatedly extruded through a polycarbonate filter of 100 nm pore size (and subsequent 30 nm pore size for ellipsometry).

The method is well established in our laboratory [25–28], and the choice of lipids offers several methodological advantages due to the long, symmetric and unsaturated acyl chains of DOPC. In particular, membrane cohesion is good, which facilitates stable, unilamellar, and largely defect-free liposomes (observed by cryo-TEM) and well defined supported lipid bilayers (observed by ellipsometry and AFM), allowing very detailed values on leakage and adsorption to be obtained. Lipid concentration was calculated from comparing CF content between batches, using the maximum leakage level.

2.7. Liposome leakage assays

Membrane permeability was measured by monitoring CF efflux from the liposomes to the external low concentration environment, resulting in loss of self-quenching and an increased fluorescence signal with excitation and emission wavelengths of 492/517 nm [29]. The fluorescence signal was measured with a SPEX Fluorolog-2 spectrofluorometer (SPEX Industries, Edison, NJ).

Measurements were conducted in 1 cm quartz cuvettes while stirring, at a fixed lipid concentration of 10 μM. In each experiment, initial signal acquisition for 10 min revealed any spontaneous leakage. The effects of each peptide concentration on the liposome systems were monitored for 30 min, at which point the initial leakage had largely subsided. The results are expressed as percent of total disruption, generated after adding of 0.05 wt.% Triton X-100 and subtracting the baseline value.

2.8. Ellipsometry

Peptide adsorption to supported lipid bilayers was studied by *in situ* null ellipsometry, using an Optrel Multiskop ellipsometer (Optrel, Kleinmachnow, Germany), equipped with a 100 mW argon laser (532 nm) at an angle of incidence of 67.66°. The adsorption was monitored using measurements of adsorption-induced changes in amplitude and phase of light reflected at the adsorbing surface. From this, the adsorbed amount was obtained according to de Feijter et al. [30], using a refractive index increment of 0.154 cm^3/g [31,32].

Corrections were routinely made to compensate for any change in bulk refractive index caused by alterations in temperature or excess electrolyte concentration. The bilayer-supporting surfaces were polished silica slides with a 30 nm thick oxide layer (Okmetic, Espoo, Finland). These were cleaned for 5 min at 80 °C in aqueous solutions of 3.6% NH_4OH and 4.3% H_2O_2, followed by 4.6% HCl and 4.3% H_2O_2. The slides were then stored in 99.7% ethanol and cleaned by plasma discharges for 5 min at 18 W in 0.2 Torr residual air prior to use, using a Harrick Plasma Cleaner PDC-32G (Harrick Plasma, Ithaca, NY). This procedure results in surfaces with an advancing contact angle against water of less than 10°, and a *z*-potential of −45 mV [33].

Prior to lipid bilayer deposition, the slides were precoated with 100 ppm polylysine for 30 min at 25 °C and subsequently rinsed with 10 mM Tris, pH 7.4. The liposomes were then added to the cuvette at a lipid concentration of 60 μM, and the resulting adsorption monitored. After liposome adsorption and fusion had stabilized, residual liposomes were removed by rinsing with Tris buffer. After lipid bilayer formation and adjustments for buffer and temperature, peptides were added cumulatively from 1/16, 1/4, 1, 4 to 16 μM, and the adsorption at each concentration monitored for 40 min (well after adsorption saturation was reached). Results presented are from duplicates of separate experiments.

2.9. Circular dichroism

Secondary structure of peptides was determined using a JASCO J810 spectropolarimeter (JASCO Corporation, Easton, MD) monitoring changes in the 200–260 nm range at 37 °C in 1 mM Tris buffer (pH 7.4), with stirring in a 1 cm quartz cuvette. Signals from the peptides, at a concentration of 8 μM, were measured in buffer alone and after 30 min of liposome incubation at a peptide:lipid ratio of 1:30. Each presented spectrum was obtained by accumulations of 15 scans at a rate of 50 nm/min. To avoid instrumental baseline drift between measurements, the background value (detected at 260 nm, where no peptide signal is present) was subtracted for each individual sample measurement. Signals were also corrected for non-peptide components, i.e., buffer and liposomes.

2.10. Liquid chromatography-mass spectrometry

LC-MS was used to detect lipids released from the supported bilayer. Samples of 500 μL were taken from the cuvette during ellipsometry measurements, both immediately prior to peptide administration and 40 min after 0.25 μM peptide administration, at which point peptide adsorption and/or lipid desorption equilibrium had been reached. The samples were freeze-dried and re-solubilized in 20 μL acetonitrile/ chloroform (1/1, v/v), and diluted with 180 μL acetonitrile/water (4/1, v/v). The *E. coli* polar lipid extract, used as reference, was prepared identically to a final concentration of 1 ng/μL. A volume of 20 μL was injected for analysis, using a Shimadzu LC10 HPLC system connected to a Thermo-Finnigan LCQ electrospray ion trap MS operated in the negative ion mode as outlined in ref. [34]. The capillary temperature was set at 210 °C and the spray voltage at 5.0 kV. Separation was done using a Waters XTerra MS C8 column (150 × 2.1 i.d. mm, 3.5 μm, 125 Å) at a flow-rate of 0.2 mL/min and by the following gradient of solvent B (100% acetonitrile) in A (50% acetonitrile in 20 mM ammonium acetate buffer, pH 6.7): 0–5 min isocratic at 5% solvent B in A; 5–20 min, 5–70% B; 20–50 min, 70–100% B, 50–59 min, isocratic at 100% B; 59–60 min, 100–5% B.

Table 1
Cytotoxic activity of kalata B1 (kB1), kalata B2 (kB2), and cycloviolacin O2 (cyO2) against U-937 GTB lymphoma, HT29 colon adenocarcinoma, and Ht116 colorectal cancer cells.

Cancer cell line	kB1 IC_{50} (μM)	kB2 IC_{50} (μM)	cyO2 IC_{50} (μM)
U-937 GTB	5.0 ± 0.7	1.7 ± 0.5	0.7 ± 1.5
HT29	14.6 ± 1.2	5.0 ± 0.3	5.3 ± 1.0
Ht116	8.2 ± 0.4	2.9 ± 0.2	1.9 ± 0.1

3. Results

3.1. Cytotoxicity

The cytotoxic effect of native cyclotides was determined using cell lines of lymphoma (U-937GTB) colorectal cancer (Ht116) and colon adenocarcinoma (HT29). As shown in Table 1, and by the concentration–response graphs provided as Supplementary Data (Fig. S1), all cyclotides showed concentration-dependent cytotoxicity in the low μM range, but with significant differences in potency between cyclotides and cell lines. Overall, cyO2 is the most potent of the cyclotides investigated, followed by kB2 and kB1. The effect was strongest against U-937 GTB, which is known to be sensitive to a wide range of cytotoxic agents.

3.2. Liposome leakage

Fig. 2 shows the leakage induced by the addition of cyclotides (0.1 to 20 μM) to liposomes of different compositions. In analogy to the cytotoxicity results, cyO2 was the most potent cyclotide against all liposomes, followed by kB2 and kB1. Liposomes containing cholesterol displayed reduced susceptibility to all cyclotides investigated, to the degree that no activity was observed for kB1 at the highest concentration tested.

CyO2 is clearly more potent against anionic DOPC/DOPA liposomes than against liposomes containing only zwitterionic DOPC, whereas kB1 and kB2 have the same or slightly less activity towards anionic liposomes compared to the zwitterionic ones. This finding suggests that membrane disruption of cyO2 is more dependent on electrostatic interactions.

These results are consistent with the higher number of positively charged residues and the positive net charge of cyO2. To investigate the impact of charge interactions, cyO2 was then subjected to chemical modifications to produce derivatives in which positive and negative charges have been neutralized, and tested against the same liposomes. These charge modifications of cyO2 have previously shown to play a key role for cytotoxic and bactericidal effects [9,12]. Thus, cyO2 derivatives containing acetylations of the two Lys residues (cyO2-Lys) and the methyl ester of the Glu residue (cyO2-Glu) were tested against anionic DOPC/DOPA liposomes. As shown in Fig. 3, leakage induced by cyO2-Lys was slightly lower than that induced by native cyO2, in line with the suggested role of charge interactions. CyO2-Glu on the other hand showed stronger lytic effect on DOPC/DOPA liposomes than native cyO2.

The order of potency of cyO2 and cyO2-Glu is contrary to the previous results of the bactericidal and cytotoxic effects of these charge derivatives [9,12]. Bearing in mind that the chosen lipid compositions are simplified models of lipid membrane compositions *in vivo*, liposomes of *E. coli* lipids were used in a follow up experiment. Notably, using *E. coli* liposomes the effect of native cyO2 increased by a factor of 50 compared to that at DOPC/DOPA, whereas the lytic activity of cyO2-Glu was identical on *E. coli* and DOPC/DOPA liposomes.

3.3. Membrane adsorption and depletion

Cyclotide adsorption on DOPC/DOPA bilayers (Fig. 4) followed the same trend as the leakage experiments. That is, the adsorption level

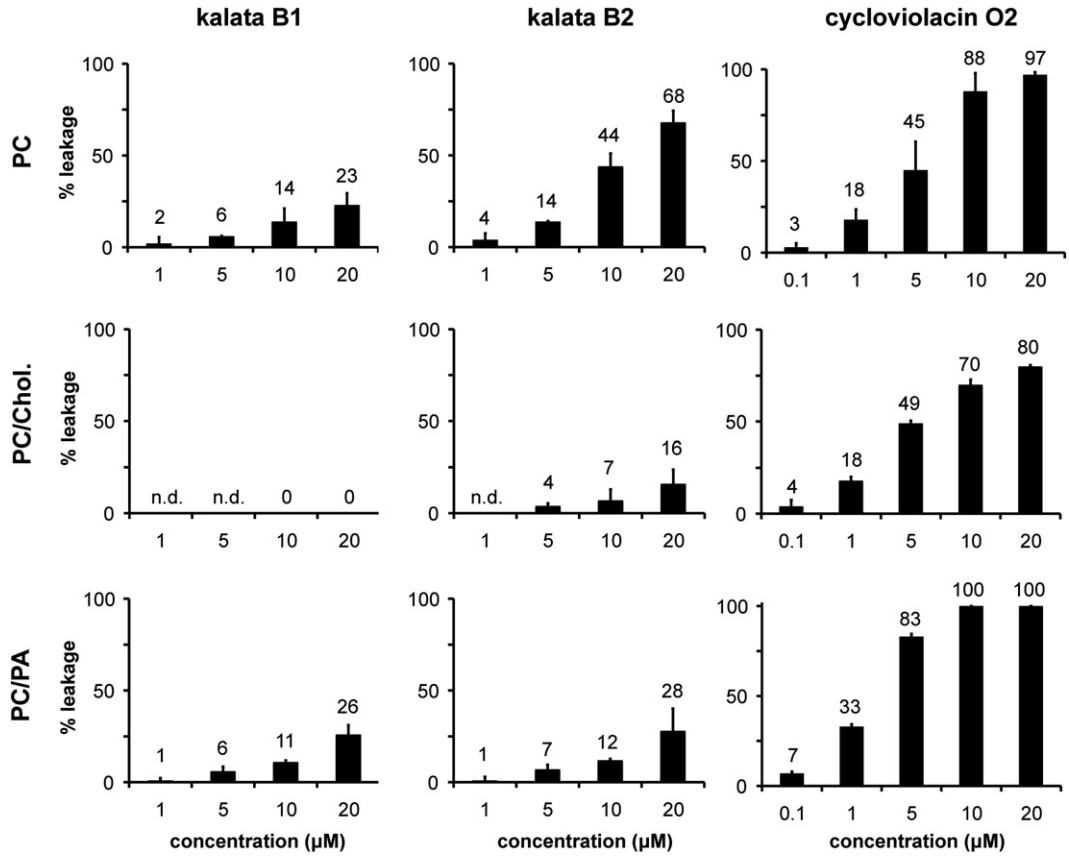

Fig. 2. Membrane-disruptive activity of native cyclotides. The graphs display percent leakage from liposomes composed of DOPC, DOPC/Cholesterol (Chol.), and DOPC/DOPA, relative to total disruption caused by the positive control Triton X-100. Experiments were performed in triplicates; error bars show standard deviations.

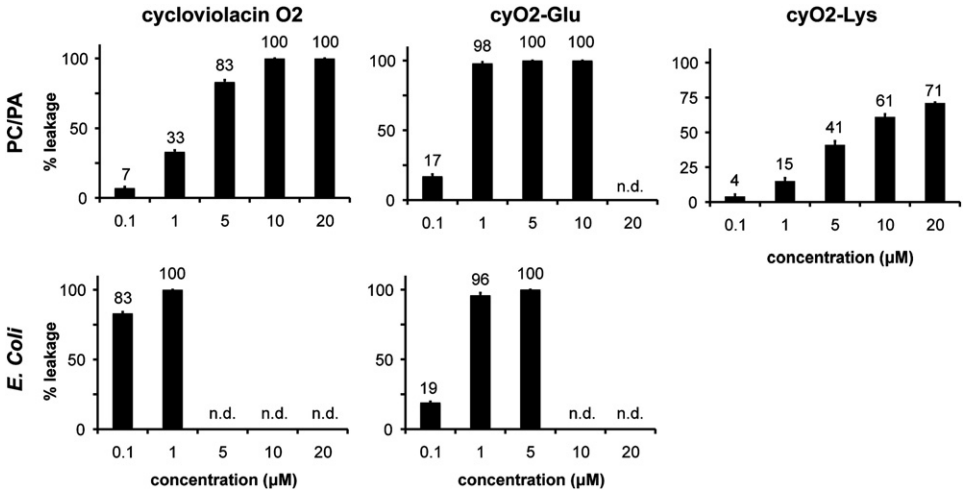

Fig. 3. Membrane-disruptive activity of native and chemically modified cycloviolacin O2 (cyO2). The graphs display percent fluorescence leakage from liposomes composed of DOPC/DOPA and E. coli polar lipid extracts, relative to total disruption caused by the positive control Triton X-100. Experiments were performed in triplicates; error bars show standard deviations.

was highest for cyO2, reaching 136 nmol/m^2 at the maximum concentration tested (16 μM). This corresponds to a peptide:lipid molar ratio of 1:35 (with an approximated surface area per lipid of 70 Å^2). KB1 and kB2 showed considerably lower adsorption, 13 nmol/m^2 and 5 nmol/m^2, respectively. Furthermore, the adsorption increased for cyO2-Glu, reaching 486 nmol/m^2, whereas cyO2-Lys displayed lower adsorption, 113 nmol/m^2, compared to the native peptide (Fig. 5). CD spectroscopy indicated that the structures of cyO2 and its derivatives were slightly more ordered in the presence of DOPC/DOPA liposomes (Fig. S2, Supplemental Data).

The adsorption of cyO2-Glu to *E. coli* membranes was similar to the adsorption to DOPC/DOPA membranes, which is in agreement with the leakage results. However, the adsorption curve for native cyO2 displayed a strikingly different profile, as shown in Fig. 6. In fact, at the lowest peptide concentration the adsorption of native cyO2 could not be determined since it caused a highly reproducible depletion of the membrane of at least 11 ± 1% of its mass, indicative of a general thinning of the bilayer and release of lipids.

LC-MS was therefore used to assay lipids released into the buffer surrounding the supported bilayer, using the lipidomic approach for *E. coli* lipids as outlined by Oursel et al. [34]. As highlighted in Fig. 7, no discernable amounts of bulk lipids could be detected prior to peptide addition. In contrast, eleven known *E. coli* lipids could be identified after peptide administration (Table 2). Two lipids in particular were overrepresented, i.e., PE-C16:0/cyC17:0 and PE-C16:0/C18:1. In the bulk, these two lipids represented 33% and 35% of the relative lipid content, respectively, which is more than twice as much as in the *E. coli* bilayer in which they represent 16% each.

4. Discussion

In the present study we demonstrate that the lytic effects of cyclotides are dependent both on their structure and the composition of the lipid membrane. Furthermore, we show that PE–lipid extraction is involved in the disruptive mechanism. The prototypic cyclotides kB1 and kB2 from the Möbius subfamily and cyO2 from the bracelet subfamily, as well as derivatives of the latter, were subjected to leakage and adsorption assays, using zwitterionic, cholesterol containing, anionic and, finally, *E. coli* membranes.

First however, the cytotoxicity of the three cyclotides was confirmed. Although we have reported the cytotoxic activity of several Möbius cyclotides before [3,20,35], this was the first time kB1 and kB2 were tested in our assay. The result was in line with previous tests: cyO2 was more potent than the Möbius cyclotides. The activity on the cellular level was matched by the order of potency using simplified human model membranes, i.e., DOPC/cholesterol liposomes: cyO2 was the most potent cyclotide followed by kB2 and kB1. Cholesterol decreased the activity for all cyclotides, and totally precluded membrane lysis by kB1 at the highest concentration tested. The condensing effect of cholesterol on membrane lipid packing results in extended alkyl chain organization, which increases

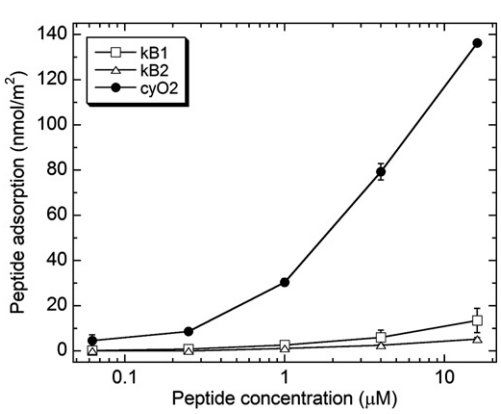

Fig. 4. Adsorption of kalata B1, B2, and cycloviolacin O2 on supported DOPC/DOPA bilayers. The experiments were conducted in 10 mM Tris buffer, pH 7.4, at 37 °C. Low adsorption was observed for kalata B1 and B2 (kB1, kB2), while cycloviolacin O2 (cyO2) displayed more extensive adsorption.

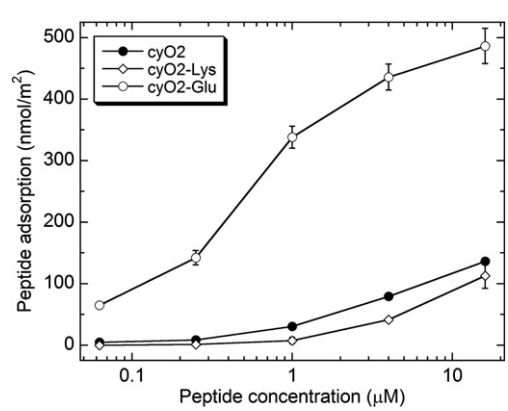

Fig. 5. Adsorption of cycloviolacin O2 variants on supported DOPC/DOPA bilayers. The experiments were conducted in 10 mM Tris buffer, pH 7.4, at 37 °C. Cycloviolacin O2 (cyO2) and its chemically modified variants (Lys and Glu) all displayed high levels of adsorption, but particularly so the cyO2-Glu variant.

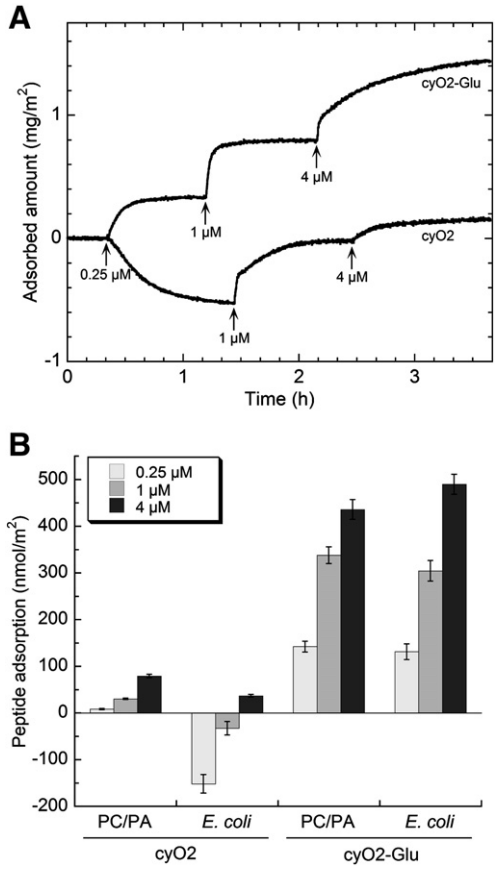

Fig. 6. Comparing adsorption for cyO2 and cyO2-Glu on DOPC/DOPA and *E. coli* bilayers. A, Representative adsorption curves by ellipsometry for cycloviolacin O2 (cyO2) and its Glu-modified variant on supported *E. coli* membranes. A decrease in membrane mass is recorded by initial cyO2 administration, followed by conventional adsorption isotherms at cumulatively increased peptide concentrations. Arrows indicate each peptide administration. B, Comparison of adsorption isotherms between cyO2 and cyO2-Glu for DOPC/DOPA and *E. coli* bilayers: the negative values were recorded with low concentrations of cyO2 on *E. coli*, as a result of membrane depletion.

bilayer thickness. It also reduces lateral density fluctuations and thereby also undulations of the bilayer [36]. These effects in turn results in reduced permeability and an increased lateral compressibility modulus, which increases deformation energy required for bilayer penetration [37,38]. As a consequence, the presence of cholesterol generally opposes peptide

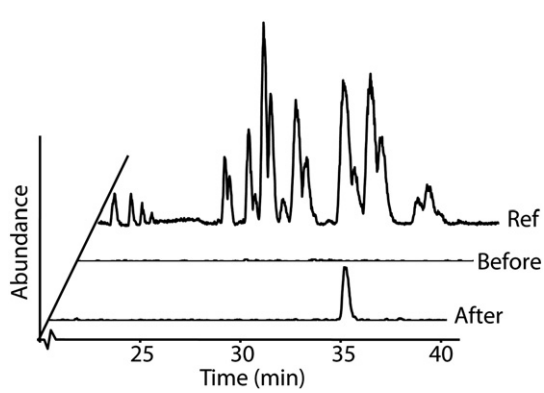

Fig. 7. LC-MS analysis of released phospholipids. The base peak ion (BPI; *m/z* 675–775) chromatogram at the top shows the reference solution (Ref) of liposomes constructed from the *E. coli* polar lipid extract. The lower two traces shows the BPI chromatograms (*m/z* 715–717) for PE C16:0/C18:1, before and after adding cycloviolacin O2 to the ellipsometry experiment. This example demonstrates that phospholipids had been released into the bulk solution. Similarly, the presence of all phospholipids that were found in the reference solution was searched for in Before/After MS traces by extracting the BPI chromatogram using their specific masses.

Table 2
CyO2-mediated lipid release from supported bilayer.

E. coli phospholipids[a]	MW	Ref (%)[b]	Extracted (%)[b]
PG-C14:0/C18:1, -C15:0/cyC17:0, -C16:0/C16:1	719	3	0
PG-C18:1/C16:1	745	2	0
PG-C16:0/cyC17:0	733	5	2
PG-C16:0/C16:0	721	1	0
PG-C16:0/C18:1	747	12	6
PG-C18:1/C18:1	773	8	4
PE-C15:0/cyC17:0, -C16:0/C16:1	688	11	5
PG-C16:0/cyC19:0	761	3	1
PE-C18:1/C16:1, -cyC17:0/cyC17:0	714	6	2
PE-C16:0/cyC17:0	702	16	33
PE-C16:0/C16:0	690	2	1
PE-C16:0/C18:1	716	16	35
PE-cyC19:0/cyC17:0, -C18:1/C18:1	742	9	7
PE-C16:0/cyC19:0,-C18:0/cyC17:0,-C17:0/C18:1	730	5	4

[a] In order of elution from RP-HPLC, other phospholipids represent <1% of the reference *E. coli* polar lipid extract.
[b] Percent of the total phospholipid composition with standard deviations less than 1.5.

adsorption and penetration into the membrane (but not necessarily the disruptive power of the actual adsorbed amount) [25]. Furthermore, cholesterol has been found to have an extremely high rate of translocation between the leaflets of the 400 bilayer [39], which is likely to have a moderating effect on peptide curvature strain influence. The tested cyclotides respond to cholesterol in a similar manner to other membrane active antimicrobial peptides [25,40].

The factor of membrane charge was then introduced to determine the effect of the relatively high net charge of cyO2 for activity. In addition, the inclusion of negatively charged DOPA to the liposomes serves to mimic bacterial membranes. CyO2 carries a net charge of $+2$ compared to ± 0 and -1 for kB1 and kB2, respectively. Hypothetically the electrostatic effect of a negatively charged membrane would confer a decrease in activity in that order. Indeed, the lytic activity of cyO2 increased for the anionic DOPC/DOPA membranes; the neutral kB1 showed essentially identical effects as against neutral DOPC liposomes; and the net negatively charged kB2 even displayed a decreased effect towards the anionic liposomes. The reduced lytic effect of cyO2-Lys towards DOPC/DOPA membranes corroborates the importance of electrostatic interactions between cyO2 and the target membrane.

For the native cyclotides, membrane adsorption followed the same pattern as the lytic activity. Thus cyO2, which displays the highest lytic potency, has highest affinity towards immobilized DOPC/DOPA membranes, whereas kB1 and kB2 both show weak lytic properties and low adsorption. In this context it is interesting to note that the orientation when binding to membranes differ for the cyclotide subfamilies [17], as a result of different locations of their main hydrophobic patch. Analysis of the surface profile of cyO2 shows that its membrane-binding hydrophobic patch stretches over loops 2 and 3, in contrast to those of kB1 and kB2, which predominantly involve loops 2, 5, and 6. Moreover, the peptides differ significantly in hydrophobicity when focusing on the solvent exposed area of each residue: net hydrophobicity is higher for cyO2 compared to kB1 and kB2 (Fig. 8A). However, adsorption to the membrane is essential for membrane-lytic activity, but the degree of lytic potency and the level of adsorption are not always proportional [25,27,28].

We then focused our studies towards the most potent cyclotide, cyO2. Prompted by the clear influence of electrostatics, and the previous results regarding structure activity relationships for its cytotoxic [12] and antibacterial effects [9], cyO2 was subjected to chemical modifications targeting the charges of Lys and Glu. CyO2-Lys, the derivative with two positively charged Lys residues masked by acetylation, showed reduced lytic effect and adsorption compared to native cyO2. These results towards DOPC/DOPA membranes corroborate the importance of electrostatic interactions between cyO2 and the target membrane.

CyO2-Glu, on the other hand, represents an increase in net positive charge by neutralization of the anionic glutamate residue, which then

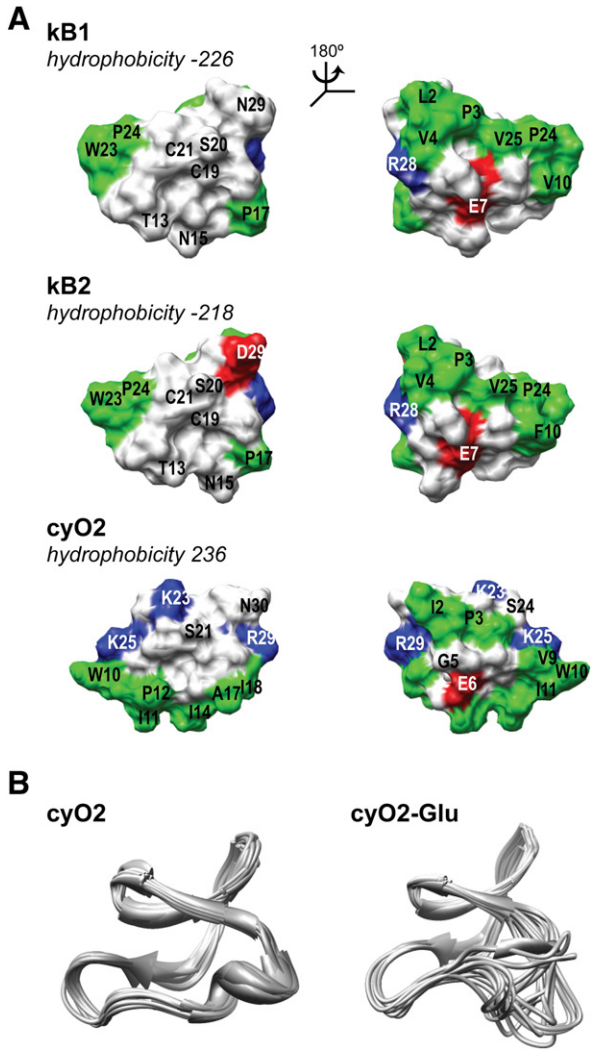

Fig. 8. Cyclotide surface hydrophobicity and structural flexibility. A, Surface representations of the Möbius cyclotides kalata B1 and B2, and the bracelet cyclotide cycloviolacin O2 (cyO2). Hydrophobic residues (Ala, Leu, Ile, Pro, Trp, Phe, and Val) are shown in green, cationic residues (Arg and Lys) in blue, anionic residues (Asp and Glu) in red, and other residues in white. Note the hydrophilc patch around the Glu residues. Peptide hydrophobicity is calculated from the sum of the Kyte–Doolittle hydropathy index [53] per percentage of each residues solvent exposure area. The latter is assessed by the MOLMOL software using structures solved by NMR (PDB ID: 2KNM, IPT4, and 1NB1). B, NMR solution structures of cyO2 (PDB ID: 2KNM) and its Glu methyl ester (PDB ID: 2KNN). The peptide backbones of the final families of 20 structures are overlaid, demonstrating the disorder/flexibility of loop 3 of cyO2-Glu.

should increase its electrostatic membrane attraction. This was also the case, the lytic activity increased slightly against DOPC/DOPA as compared to the native peptide, but the adsorption increased dramatically. That increase made it reasonable to assume that additional structural differences may contribute.

In fact, esterification of Glu has been shown to break internal hydrogen bonds that stabilize the cyclotide structure, in particular the helical loop 3 that is tied to the core of the peptide through those bonds [12,41]. Disruption of that loop causes decreased cytotoxic [12,41] and antibacterial [9] activities (on bacteria with similar lipid compositions as our *E. coli* model [42]). However, using DOPC/DOPA liposomes the effect was the opposite, i.e., destabilization of the structure rendered the peptide more membrane active.

Strikingly, using *E. coli* liposomes, the order of potency for cyO2 and cyO2-Glu was reversed. Although cyO2-Glu displayed the same activity for both types of lipid compositions, the potency of native cyO2 increased by a factor of 50. In that context, it should be noted that liposomes of DOPC/DOPA and *E. coli* lipids have similar charge densities both in terms of anionic composition and zeta-potential [27,28]. Hence, in addition to membrane charge density and cholesterol content, cyclotide membrane disruption also depends on the finer details of cyclotide–membrane interactions.

A previous study [41] of the structural aspects of cyO2-Glu revealed that the modification leads to relaxation of loop 3, followed by increased flexibility (Fig. 8B). In fact, this may contribute to adsorption: relaxation of an alpha helix confers higher adsorption levels if that structure again is stabilized by the interaction with the lipid membrane [43,44]. That transition can be followed by e.g. CD spectroscopy. But because of the complexity of the CD spectra for such highly knotted structures as cyclotides, the degree of helix induction by adsorption could not be quantified with certainty. However qualitatively, the CD spectra for the cyO2 variants indicated that the amount of ordered structures increased upon membrane binding due to helix formation. This effect was more pronounced for cyO2-Glu compared to its analogues, indicating that this is an adsorption discriminating factor.

Other possible contributing factors may be that an unorganized hydrophobic loop 3 either associate more closely with the rest of the hydrophobic patch (e.g. loop 2) due to a higher flexibility and thus render the cyclotide more amphiphilic, or facilitate interaction with the membrane interior and anchoring the peptide in a more energetically favourable way.

CyO2-Glu shows essentially identical leakage inducing properties towards the anionic DOPC/DOPA and *E. coli* liposomes, while native cyO2 is about 50 times as potent against the latter. This suggests that membrane lysis by cyO2 is sensitive towards variations either in the specific compositions of the alkyl groups (pure unsaturated dioleoyl C18:1 vs. ~50% saturated C16:0 and C14:0; ~50% unsaturated C18:1 and C16:1) or to the phosphatidyl groups (choline and acid *vs.* ethanolamine and glycerides). The nature of the sensitivity observed, is neither directly related to the overall membrane charge nor to the presence of liquid order phase. This specificity was supported by ellipsometry data using *E. coli* liposomes: native cyO2 gave a decrease in membrane mass with the initial peptide administration, followed by conventional adsorption isotherms with cumulatively increased peptide concentrations. Using LC-MS, we were able to demonstrate that certain PE-lipids are extracted from the membrane. Since the depletion of the membrane was shown to be a smooth process over time with a high degree of reproducibility between triplicate experiments, and with subsequent stabile isotherms, the mechanism involved is likely not sudden detachment of large membrane patches. More likely, the process involves a diffuse process of PE-specific micellisation of peptide–lipid complexes over the entire membrane surface.

The loss of mass from the bilayer represents at least 11%, which must leave a significant contribution to membrane leakage. In the case of cyO2, membrane depletion is most likely due to peptide–lipid rather than peptide–peptide interactions because of the following reasons: firstly, depletion is primarily observed at low concentration of cyO2, opposite to expectations from concentration-dependent peptide oligomerisation. Secondly, the loss of mass is specific for the membrane composition and independent of the electrostatics of the membrane. This peptide–lipid interaction responsible for the observed membrane depletion can be direct, i.e. lipid specific affinity for the peptide, or indirect, i.e. curvature stress dependent demixing of lipids which by lipid packing factors energetically favour peptide accumulation within specific patches. PE-lipids normally have a negative curvature contribution to the membrane. As such, they are beneficial for balancing curvature stress from an interfacial expanding peptide (i.e., a peptide that contributes to positive curvature as a consequence of shallow penetration). This may explain the preferential extraction of certain PE lipids, since they are the phospholipids expected to associate with the peptide microenvironment within the membrane and therefore more likely to be incorporated in detached aggregates, rather than lipids of more positive packing parameters. If

the component extraction is driven by a phospholipid-specific affinity due to peptide structure and electrochemical properties, or demixing by means of curvature effects alone, remains to be shown.

In either case, the specific peptide lipid interaction puts a new angle on the proposed pore forming model of cyclotides [18,19]. That proposed mechanism is dependent on peptide–peptide interactions exploiting a "bioactive face", i.e., the hydrophilic patch around the conserved Glu residue (Fig. 8). Judged from the results in the current study, that patch is instead involved in the interaction with PE-lipids to directly or indirectly contribute to membrane depletion.

When placing the preferential extraction of PE in perspective, it is noteworthy that several unrelated proteins and peptides are known to bind PE with various degrees of selectivity. These include the family of phosphatidylethanolamine (PE)-binding proteins (PEBPs) [45], the lanthionine-containing peptide antibiotics, e.g., duramycin [46], and recently the oligomeric amyloid-beta peptide (Abeta) that seem to preferentially bind to PE [47]. The preferential binding of Abeta to PE lipids may reflect a similar preference of other amyloid peptides. For example, the amyloidogenic peptide islet amyloid polypeptide (IAPP, also known as amylin) has been suggested to facilitate the formation of torodial pores by induction of excess membrane curvature [48]. In these cases it seems that PE-binding play a role for peptide adhesion to the membrane (PEBPs and Abeta), or, in the case of duramycin, membrane destabilization. In addition, kalata B1 and B6 have also been shown to have high affinity towards PE-containing immobilized liposomes, using surface plasmon resonance [14]. To our knowledge, actual extraction of specific membrane components similar to what was observed for cyO2 in the current work is limited to the example of cyclodextrin and cholesterol [49,50].

It is becoming evident that membrane interactions are central for the biological effects of cyclotides. The results of the present study underpin a mechanism involving lipid depletion followed by lysis, which provides a plausible mechanism of action for the bactericidal [9] effect of cyO2. The same mechanism may explain the cytotoxic [13] and insecticidal [51] effects of cyclotides: microscopy studies have shown that these events include disruption of the cell membrane; in the case of the insecticidal activity, it has also been shown that insect gut cell disruption is preceded by blebbing and swelling. However, there are reasons to believe that different cyclotides may have different modes of action. For example, a recent study of kB1 suggested formation of multimeric pores in the membrane [18], and the cyclotide like peptide MCoTI-II has been shown to cross the cell membrane by micropinocytosis [52]. The extraction of PE-lipids is of particular interest since it may be used as a factor to control specificity: the outer leaflet of human cell membranes displays low concentrations of PE-lipids as compared to most bacteria. In the case of cyO2-Glu and the native cyO2, the data presented here indicate that their lytic activity is partly mediated by different mechanisms; the former purely by adsorption induced stress while the latter also by increasing membrane susceptibility to that stress by a phospholipid-specific depletion.

In conclusion, size and distribution of the hydrophobic surface, net cationic charge, and the intramolecular hydrogen bonding potential of the cyclotide, are all factors that influence membrane adsorption and disruption of cyclotides. The magnitude of the individual contribution of these factors is in turn governed by lipid membrane composition, in terms of cholesterol and anionic composition. More surprisingly, we identified a unique feature of the bracelet cyclotide cycloviolacin O2: the ability of the native peptide to selectively target and destroy membranes composed of *E. coli* lipids by a mechanism that includes membrane depletion by PE-preferential extraction, and suggests that membrane thinning precedes lysis. In fact, cyO2 was 100-fold more potent when tested against *E. coli* membranes than towards the cholesterol containing DOPC membranes, which represent the standard model for human cell membranes in our model system. Albeit there is no comparative study of this selectivity *in vivo* (i.e., the effect against *E. coli* vs. the effects on human cells in a comparable experimental setting) the current work represents a potential turning point for our view on cyclotides as antimicrobial agents.

Supplementary materials related to this article can be found online at 10.1016/j.bbamem.2011.07.004.

Acknowledgments

We thank Drs. Joachim Gullbo and Jenny Felth for help with cytotoxicity tests, and Lotta Wahlberg and Dr. Lovisa Ringstad for technical assistance with lipid bilayers. UG is supported by the Swedish Research Council (#621-2007-5167), and the Swedish Foundation for Strategic Research (#F06-0058). MM acknowledges support from the Swedish Research Council (#621-2009-3009).

References

[1] D.J. Craik, N.L. Daly, T. Bond, C. Waine, Plant cyclotides: a unique family of cyclic and knotted proteins that defines the cyclic cystine knot structural motif, J. Mol. Biol. 294 (1999) 1327–1336.
[2] M.L. Colgrave, D.J. Craik, Thermal, chemical, and enzymatic stability of the cyclotide kalata B1: the importance of the cyclic cystine knot, Biochemistry 43 (2004) 5965–5975.
[3] P. Lindholm, U. Göransson, S. Johansson, P. Claeson, J. Gullbo, R. Larsson, L. Bohlin, A. Backlund, Cyclotides: a novel type of cytotoxic agents, Mol. Cancer Ther. 1 (2002) 365–369.
[4] D.C. Ireland, M.L. Colgrave, D.J. Craik, A novel suite of cyclotides from *Viola odorata*: sequence variation and the implications for structure, function and stability, Biochem. J. 400 (2006) 1–12.
[5] N.L. Daly, D.J. Craik, Acyclic permutants of naturally occurring cyclic proteins. Characterization of cystine knot and beta-sheet formation in the macrocyclic polypeptide kalata B1, J. Biol. Chem. 275 (2000) 19068–19075.
[6] K.R. Gustafson, R.C. Sowder, L.E. Henderson, I.C. Parsons, Y. Kashman, J.H. Cardellina, J.B. McMahon, L.K. Buckheit, L.K. Pannell, M.R. Boyd, Circulins A and B. Novel human immunodeficiency virus (HIV)-inhibitory macrocyclic peptides from the tropical tree *Chassalia parvifolia*, J. Am. Chem. Soc. 116 (1994) 9337–9338.
[7] M.L. Colgrave, A.C. Kotze, D.C. Ireland, C.K. Wang, D.J. Craik, The anthelmintic activity of the cyclotides: natural variants with enhanced activity, Chembiochem 9 (2008) 1939–1945.
[8] U. Göransson, M. Sjögren, E. Svangård, P. Claeson, L. Bohlin, Reversible antifouling effect of the cyclotide cycloviolacin O2 against barnacles, J. Nat. Prod. 67 (2004) 1287–1290.
[9] M. Pränting, C. Lööv, R. Burman, U. Göransson, D.I. Andersson, The cyclotide cycloviolacin O2 from *Viola odorata* has potent bactericidal activity against Gram-negative bacteria, J. Antimicrob. Chemother. 65 (2010) 1964–1971.
[10] J.P. Tam, Y.A. Lu, J.L. Yang, K.W. Chiu, An unusual structural motif of antimicrobial peptides containing end-to-end macrocycle and cystine-knot disulfides, Proc. Natl. Acad. Sci. U.S.A. 96 (1999) 8913–8918.
[11] C. Jennings, J. West, C. Waine, D. Craik, M. Anderson, Biosynthesis and insecticidal properties of plant cyclotides: the cyclic knotted proteins from *Oldenlandia affinis*, Proc. Natl. Acad. Sci. U.S.A. 98 (2001) 10614–10619.
[12] A. Herrmann, E. Svangård, P. Claeson, J. Gullbo, L. Bohlin, U. Göransson, Key role of glutamic acid for the cytotoxic activity of the cyclotide cycloviolacin O2, Cell. Mol. Life Sci. 63 (2006) 235–245.
[13] E. Svangård, R. Burman, S. Gunasekera, H. Lövborg, J. Gullbo, U. Göransson, Mechanism of action of cytotoxic cyclotides: cycloviolacin O2 disrupts lipid membranes, J. Nat. Prod. 70 (2007) 643–647.
[14] H. Kamimori, K. Hall, D.J. Craik, M.I. Aguilar, Studies on the membrane interactions of the cyclotides kalata B1 and kalata B6 on model membrane systems by surface plasmon resonance, Anal. Biochem. 337 (2005) 149–153.
[15] Z.O. Shenkarev, K.D. Nadezhdin, E.N. Lyukmanova, V.A. Sobol, L. Skjeldal, A.S. Arseniev, Divalent cation coordination and mode of membrane interaction in cyclotides: NMR spatial structure of ternary complex Kalata B7/Mn2+/DPC micelle, J. Inorg. Biochem. 102 (2008) 1246–1256.
[16] Z.O. Shenkarev, K.D. Nadezhdin, V.A. Sobol, A.G. Sobol, L. Skjeldal, A.S. Arseniev, Conformation and mode of membrane interaction in cyclotides. Spatial structure of kalata B1 bound to a dodecylphosphocholine micelle, FEBS J. 273 (2006) 2658–2672.
[17] C.K. Wang, M.L. Colgrave, D.C. Ireland, Q. Kaas, D.J. Craik, Despite a conserved cystine knot motif, different cyclotides have different membrane binding modes, Biophys. J. 97 (2009) 1471–1481.
[18] Y.H. Huang, M.L. Colgrave, N.L. Daly, A. Keleshian, B. Martinac, D.J. Craik, The biological activity of the prototypic cyclotide kalata B1 is modulated by the formation of multimeric pores, J. Biol. Chem. 284 (2009) 20699–20707.
[19] S.M. Simonsen, L. Sando, K.J. Rosengren, C.K. Wang, M.L. Colgrave, N.L. Daly, D.J. Craik, Alanine scanning mutagenesis of the prototypic cyclotide reveals a cluster of residues essential for bioactivity, J. Biol. Chem. 283 (2008) 9805–9813.
[20] A. Herrmann, R. Burman, J.S. Mylne, G. Karlsson, J. Gullbo, D.J. Craik, R.J. Clark, U. Göransson, The alpine violet Viola biflora, is a rich source of cyclotides with potent cytotoxicity, Phytochemistry 69 (2008) 939–952.
[21] D.F. Hunt, J.R. Yates III, J. Shabanowitz, S. Winston, C.R. Hauer, Protein sequencing by tandem mass spectrometry, Proc. Natl. Acad. Sci. U.S.A. 83 (1986) 6233–6237.

[22] K.L. Gudiksen, I. Gitlin, J. Yang, A.R. Urbach, D.T. Moustakas, G.M. Whitesides, Eliminating positively charged lysine epsilon-NH3+ groups on the surface of carbonic anhydrase has no significant influence on its folding from sodium dodecyl sulfate, J. Am. Chem. Soc. 127 (2005) 4707–4714.
[23] R. Larsson, P. Nygren, A rapid fluorometric method for semiautomated determination of cytotoxicity and cellular proliferation of human tumor cell lines in microculture, Anticancer Res. 9 (1989) 1111–1119.
[24] E. Lindhagen, P. Nygren, R. Larsson, The fluorometric microculture cytotoxicity assay, Nat. Protoc. 3 (2008) 1364–1369.
[25] P. Wessman, A.A. Strömstedt, M. Malmsten, K. Edwards, Melittin–lipid bilayer interactions and the role of cholesterol, Biophys. J. 95 (2008) 4324–4336.
[26] A. Strömstedt, L. Ringstad, A. Schmiidtchen, M. Malmsten, Interaction between amphipathic peptides and phospholipid membranes, Curr. Opin. Colloid In. (2010).
[27] A.A. Strömstedt, M. Pasupuleti, A. Schmidtchen, M. Malmsten, Oligotryptophan-tagged antimicrobial peptides and the role of the cationic sequence, Biochim. Biophys. Acta 1788 (2009) 1916–1923.
[28] A.A. Strömstedt, P. Wessman, L. Ringstad, K. Edwards, M. Malmsten, Effect of lipid headgroup composition on the interaction between melittin and lipid bilayers, J. Colloid Interface Sci. 311 (2007) 59–69.
[29] R.F. Chen, J.R. Knutson, Mechanism of fluorescence concentration quenching of carboxyfluorescein in liposomes: energy transfer to nonfluorescent dimers, Anal. Biochem. 172 (1988) 61–77.
[30] A. De Feijter, J. Benjamins, F.A. Veer, Ellipsometry as a tool to study the adsorption behavior of synthetic and biopolymers at the air–water interface, Biopolymers 17 (1978) 1758–1772.
[31] F. Tiberg, I. Harwigsson, M. Malmsten, Formation of model lipid bilayers at the silica-water interface by co-adsorption with non-ionic dodecyl maltoside surfactant, Eur. Biophys. J. 29 (2000) 196–203.
[32] H.P. Vacklin, F. Tiberg, R.K. Thomas, Formation of supported phospholipid bilayers via co-adsorption with beta-D-dodecyl maltoside, Biochim. Biophys. Acta 1668 (2005) 17–24.
[33] M. Malmsten, N. Burns, A. Veide, Electrostatic and hydrophobic effects of oligopeptide insertions on protein adsorption, J. Colloid Interface Sci. 204 (1998) 104–111.
[34] D. Oursel, C. Loutelier-Bourhis, N. Orange, S. Chevalier, V. Norris, C.M. Lange, Lipid composition of membranes of *Escherichia coli* by liquid chromatography/tandem mass spectrometry using negative electrospray ionization, Rapid Commun. Mass Spectrom. 21 (2007) 1721–1728.
[35] E. Svangård, U. Göransson, Z. Hocaoglu, J. Gullbo, R. Larsson, P. Claeson, L. Bohlin, Cytotoxic cyclotides from Viola tricolor, J. Nat. Prod. 67 (2004) 144–147.
[36] J. Henriksen, A.C. Rowat, J.H. Ipsen, Vesicle fluctuation analysis of the effects of sterols on membrane bending rigidity, Eur. Biophys. J. 33 (2004) 732–741.
[37] D. Needham, R.S. Nunn, Elastic deformation and failure of lipid bilayer membranes containing cholesterol, Biophys. J. 58 (1990) 997–1009.
[38] J.M. Smaby, M.M. Momsen, H.L. Brockman, R.E. Brown, Phosphatidylcholine acyl unsaturation modulates the decrease in interfacial elasticity induced by cholesterol, Biophys. J. 73 (1997) 1492–1505.
[39] Y. Lange, J. Dolde, T.L. Steck, The rate of transmembrane movement of cholesterol in the human erythrocyte, J. Biol. Chem. 256 (1981) 5321–5323.
[40] A. Ramamoorthy, D.K. Lee, T. Narasimhaswamy, R.P. Nanga, Cholesterol reduces pardaxin's dynamics-a barrel-stave mechanism of membrane disruption investigated by solid-state NMR, Biochim. Biophys. Acta 1798 (2010) 223–227.
[41] U. Göransson, A. Herrmann, R. Burman, L.M. Haugaard-Jonsson, K.J. Rosengren, The conserved glu in the cyclotide cycloviolacin O2 has a key structural role, Chembiochem 10 (2009) 2354–2360.
[42] A. Aloui, M. Mihoub, M.M. Sethom, A. Chatti, M. Feki, N. Kaabachi, A. Landoulsi, Effects of dam and/or seqA mutations on the fatty acid and phospholipid membrane composition of *Salmonella enterica* serovar Typhimurium, Foodborne Pathog. Dis. 7 (2010) 573–583.
[43] T. Wieprecht, O. Apostolov, M. Beyermann, J. Seelig, Thermodynamics of the alpha-helix-coil transition of amphipathic peptides in a membrane environment: implications for the peptide–membrane binding equilibrium, J. Mol. Biol. 294 (1999) 785–794.
[44] T. Wieprecht, M. Beyermann, J. Seelig, Thermodynamics of the coil-alpha-helix transition of amphipathic peptides in a membrane environment: the role of vesicle curvature, Biophys. Chem. 96 (2002) 191–201.
[45] M.J. Banfield, J.J. Barker, A.C. Perry, R.L. Brady, Function from structure? The crystal structure of human phosphatidylethanolamine-binding protein suggests a role in membrane signal transduction, Structure 6 (1998) 1245–1254.
[46] M. Rzeznicka II, E.H. Sovago, M. Backus, T. Bonn, T. Yamada, M. Kobayashi, Kawai, Duramycin-induced destabilization of a phosphatidylethanolamine monolayer at the air-water interface observed by vibrational sum-frequency generation spectroscopy, Langmuir 26 (2010) 16055–16062.
[47] E. Cazzaniga, A. Bulbarelli, E. Lonati, A. Orlando, F. Re, M. Gregori, M. Masserini, Abeta peptide toxicity is reduced after treatments decreasing phosphatidylethanolamine content in differentiated neuroblastoma cells, Neurochem. Res. 36 (2011) 863–869.
[48] P.E. Smith, J.R. Brender, A. Ramamoorthy, Induction of negative curvature as a mechanism of cell toxicity by amyloidogenic peptides: the case of islet amyloid polypeptide, J. Am. Chem. Soc. 131 (2009) 4470–4478.
[49] Y. Ohtani, T. Irie, K. Uekama, K. Fukunaga, J. Pitha, Differential effects of alpha-, beta- and gamma-cyclodextrins on human erythrocytes, Eur. J. Biochem. 186 (1989) 17–22.
[50] S. Ilangumaran, D.C. Hoessli, Effects of cholesterol depletion by cyclodextrin on the sphingolipid microdomains of the plasma membrane, Biochem. J. 335 (Pt 2) (1998) 433–440.
[51] B.L. Barbeta, A.T. Marshall, A.D. Gillon, D.J. Craik, M.A. Anderson, Plant cyclotides disrupt epithelial cells in the midgut of lepidopteran larvae, Proc. Natl. Acad. Sci. U.S.A. 105 (2008) 1221–1225.
[52] K.P. Greenwood, N.L. Daly, D.L. Brown, J.L. Stow, D.J. Craik, The cyclic cystine knot miniprotein MCoTI-II is internalized into cells by macropinocytosis, Int. J. Biochem. Cell Biol. 39 (2007) 2252–2264.
[53] J. Kyte, R.F. Doolittle, A simple method for displaying the hydropathic character of a protein, J. Mol. Biol. 157 (1982) 105–132.